RESEARCH HIGHLIGHTS

Journal of Semiconductors
(2022) 43, 060201
doi: 10.1088/1674-4926/43/6/060201

Large-area organic solar cells

Min Li[1], Jilin Wang[3, †], Liming Ding[2, †], and Xiaoyan Du[1, †]

[1]School of Physics, Shandong University, Jinan 250100, China

[2]Center for Excellence in Nanoscience (CAS), Key Laboratory of Nanosystem and Hierarchical Fabrication (CAS), National Center for Nanoscience and Technology, Beijing 100190, China

[3]School of Materials Science and Engineering, Key Laboratory of New Processing Technology for Nonferrous Metals and Materials (MoE), Guilin University of Technology, Guilin 541004, China

Citation: M Li, J L Wang, L M Ding, and X Y Du, Large-area organic solar cells[J]. *J. Semicond.*, 2022, 43(6), 060201. https://doi.org/10.1088/1674-4926/43/6/060201

Organic solar cells (OSCs) have made significant progress due to the fast advances in nonfullerene acceptors (NFAs) since 2015[1–7]. The power conversion efficiency (PCE) for small-area single-junction OSCs is around 19% with an active area <0.1 cm^2[8–11]. Scalability is a key factor in developing this technology. When scaling lab cells to large-area modules, the device performance might drop. Brabec *et al.* proposed a stage–gate process for OSCs from R&D effort to commercialization, which includes materials development, processing, prototyping, pilot process and upscaling[12]. Lab-to-fab transfer involves processing environment (glovebox or ambient air), coating technique (spin coating or scalable techniques), device size (<1, 1–200, or >200 cm^2), device type (cells or modules), top electrode (evaporated or printed) and solvent (halogenated or green). To visualize the upscaling losses, representative high-efficiency lab cells with small active areas and those single cells and modules with active area over 1 cm^2 reported from 2018 to 2021 are summarized in Fig. 1(a) and Table 1. In addition, the records in NREL's Champion Module Efficiencies Chart are also included for comparison[13]. The PCE usually declines with the increase of the active area of the devices.

The representative high-performance solar modules with active area over 1 cm^2 are presented in Fig. 1. The chemical structures for the photoactive materials are shown in Fig. 1(b). In 2020, Huang *et al.* designed a nonfullerene acceptor named DTY6, and PM6:DTY6 module (area 18 cm^2) gave a PCE of 14.45% (certified 13.98%) (Fig. 1(c))[14]. Very recently, Zhou *et al.* found that the long side chain of BTP-eC9 inhibited excessive aggregation when processed with chlorobenzene (CB), and PM6:BTP-eC9 module offered a PCE of 14.07% with a wide processing window (area 25 cm^2) (Fig. 1(d))[15]. Li *et al.* reported a Y6 derivative named BTO, and PM6:Y6:BTO:$PC_{71}BM$ module gave a PCE of 14.26% (area 36 cm^2), which was realized without thermal annealing and with non-halogenated processing solvent. It is the record for OSC modules with an active area exceeding 20 cm^2 (Fig. 1(e))[16].

The efficiency loss for solar modules relates to the change of processing method and increase of area[17]. Spin-coating is a common method for making lab cells, but not suitable for making large-area modules[18]. Slot-die coating is one of the most practical coating techniques for solar modules. In 2020, Wei *et al.* used slot-die coating to make PTB7-Th:CO$_i$8DFIC:$PC_{71}BM$ ternary devices, achieving PCEs of 12.16% and 10.09% for 1 and 25 cm^2 flexible devices, respectively (Fig. 2(a))[19]. Environmental-friendly manufacturing requires non-toxic solvents, also leading to PCE loss due to limited solubility of the active materials[20]. Side-chain engineering is an effective approach to optimize active-layer morphology and attain high-performance organic photovoltaic (OPV) modules.

The geometrical fill factor (GFF), defined as the ratio of active area and module area, needs to be considered when evaluating the upscaling loss in PCE. In 2020, Egelhaaf *et al.* optimized laser patterning parameters and the number of cells in the module for high GFF with minimum PCE loss. The certified PCEs were 12.6% for 26 cm^2 module and 11.7% for 204 cm^2 module. The GFF was over 95% (Fig. 2(b))[21]. Before this report, the record efficiency 8.7% for OPV module (802 cm^2) was demonstrated by Toshiba.

For large area and low cost, all functional layers should be processed *via* solution coating. PEDOT:PSS is commonly used with metal grid as electrode, but its transmittance is weak in the spectral region over 600 nm, which is of great importance to the absorption of the active layer[22]. Recently, Zhou *et al.* made a solution-processed composite electrode Ag-NWs:PEI-Zn and it presented low roughness, high transmittance and good thermal stability. A 54 cm^2 flexible module with a 13.2% PCE was obtained (Fig. 2(c))[23]. However, the top MoO_x/Ag layer was still thermally evaporated. In 2019, evaporation-free flexible OSC modules offered a PCE of 5.25% on an active area of 80 cm^2[24]. In 2021, Egelhaaf *et al.* developed a printable silver-nanoparticle (AgNP) film as top electrode and achieved a similar performance as the evaporated ones. The maximum PCE for 4 cm^2 modules with AgNP electrode was 7%[25]. Great efforts are still needed to realize all-solution processed efficient OPV modules.

In short, large-area OSCs have made inspiring advances with the development of novel materials and processing techniques. Efforts are needed to improve the scalability of OSCs and achieve large-area, low-cost, environmental-friendly and all-layer-printed modules.

Acknowledgements

X. Du thanks National Natural Science Foundation of China (52103222), Natural Science Foundation of Shandong Province (ZR2021QA009), Taishan Scholar Foundation of Shan-

Correspondence to: J L Wang, jilinwang@glut.edu.cn; L M Ding, ding@nanoctr.cn; X Y Du, duxy@sdu.edu.cn
Received 5 APRIL 2022.

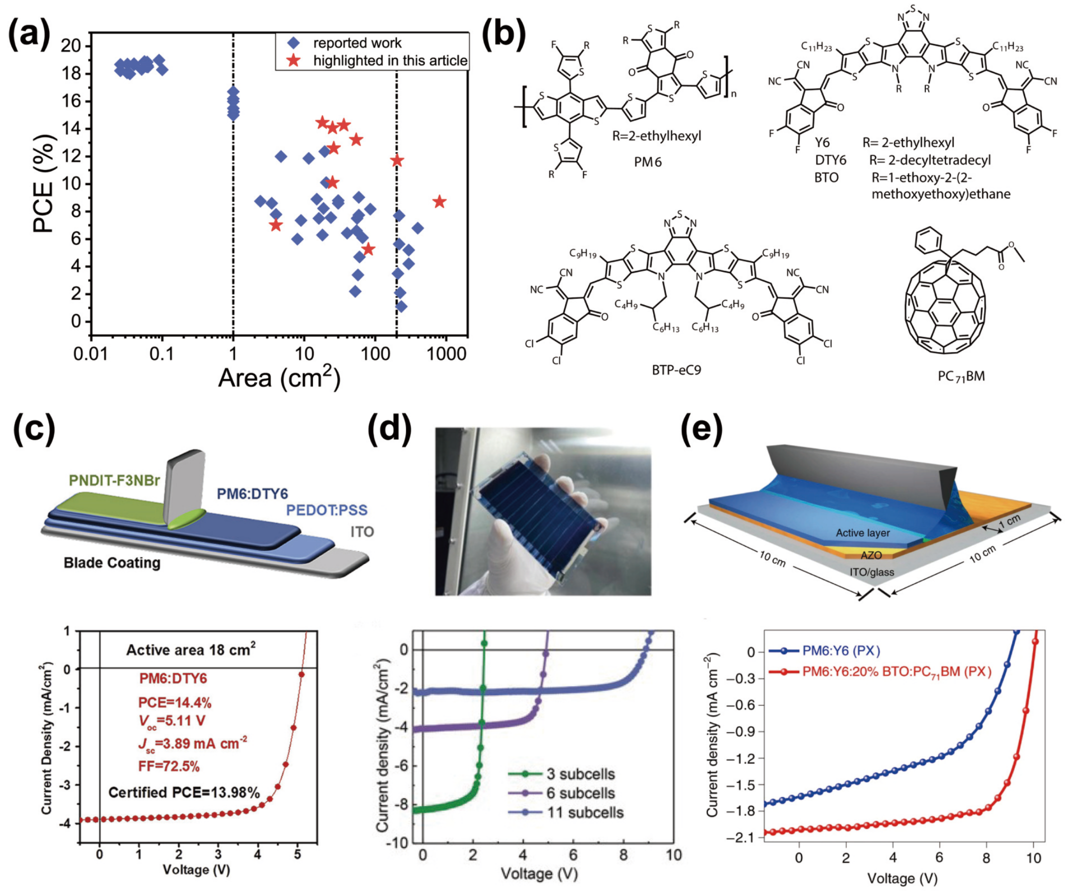

Fig. 1. (Color online) (a) The PCEs for lab cells with small areas and for devices and modules with active area over 1 cm^2 (2018–2021); the records in NREL's Champion Module Efficiencies Chart are included for comparison. (b) The chemical structures for the active materials. (c) Schematic for the device structure and *J*–*V* curves for 18 cm^2 module with a PCE of 14.45% (certified 13.98%). Reproduced with permission[14], Copyright 2020, Elsevier. (d) 25.21 cm^2 module; *J*–*V* curve changes with number of subcells. Reproduced with permission[15], Copyright 2021, Wiley. (e) Schematic for the blade-coating process and *J*–*V* curves for modules with different active layers. Reproduced with permission[16], Copyright 2021, Springer Nature.

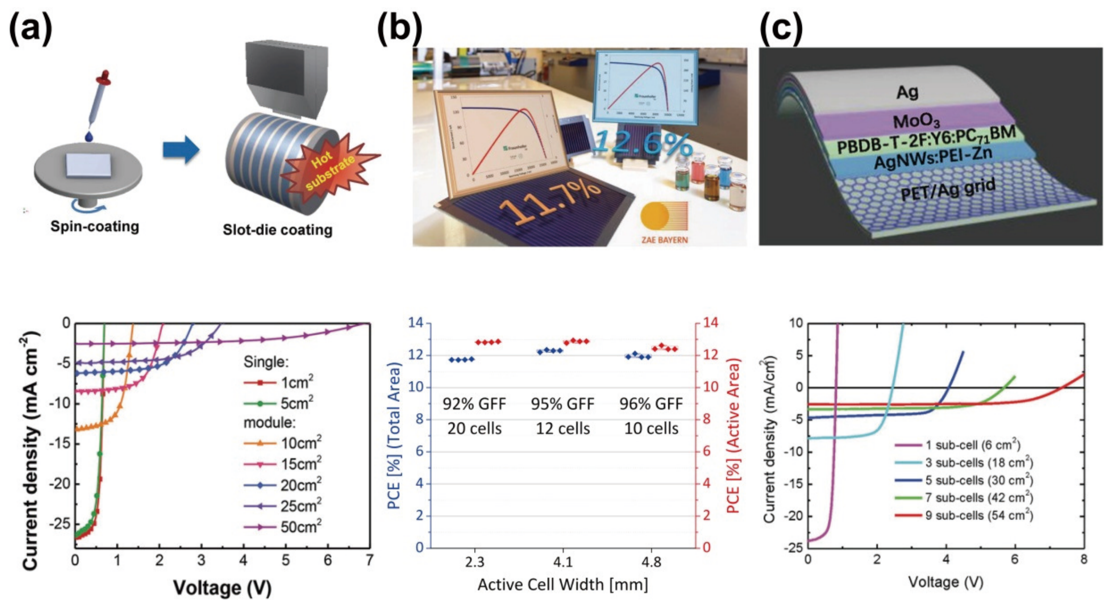

Fig. 2. (Color online) (a) Schematic for spin coating and slot-die coating (top) and *J*–*V* curves for single cells and modules with different active area (bottom). Reproduced with permission[19], Copyright 2020, Wiley. (b) Photos and *J*–*V* curves for 26 cm^2 module (PCE 12.6%) and 204 cm^2 module (PCE 11.7%) (top) certified by Fraunhofer ISE. Reproduced with permission[12], Copyright 2020, Wiley. PCE changes with active cell width. Reproduced with permission [21], Copyright 2020, Wiley. (c) Schematic for the device structure; *J*–*V* curves change with the number of subcells (module area is up to 54 cm^2). Reproduced with permission[23], Copyright 2021, Wiley.

Table 1. The representative single cells and modules with active area over 1 cm^2 (2018–2021). The records in NREL's Champion Module Efficiencies Chart are also included.

Area (cm^2)	Year	PCE (%)	Active layer	Solvent	Coating	Ref.
1	2020	16	PBDB-TF:BTP-4Cl-16	chlorobenzene	Spin-coating	[26]
1	2020	15.5	PBDB-TF:BTP-4Cl-16	chlorobenzene	Blade-coating	[26]
1	2021	15	PTzBI-oF:PM6:PFA1	chloroform	Spin-coating	[27]
1	2021	16.71	PBDB-TF:BTP-eC9	chloroform	Spin-coating	[28]
1	2021	16.2	PBDB-TF:BTP-eC9	chloroform	Blade-coating	[29]
1.015	2021	15.24	D18:Y6	chloroform	Spin-coating	[30]
4	2021	7	PV2000:$PC_{61}BM$	*o*-xylene	Slot-die coating	[25]
9	2019	7.35	PBDB-T:ITIC	chlorobenzene	Spin-coating	[31]
11.52	2020	11.86	PM6:Y6	chloroform	Blade-coating	[32]
15	2019	8.90	PBDB-T:ITIC	chlorobenzene	Slot-die printing	[33]
16	2018	7.50	PTB7-Th:$PC_{71}BM$	2-methylanisole	Blade-coating	[34]
18	2020	14.45	PM6:DTY6	*o*-xylene	Blade-coating	[14]
18	2018	6.30	PBDB-T:ITIC	chlorobenzene	Maobi-coating	[35]
18.63	2021	8.22	PTB7:$PC_{71}BM$	chlorobenzene	Spin-coating	[36]
19.34	2021	12.36	PM6:Y6:ITIC:$PC_{71}BM$	chloroform	Spin-coating	[37]
20.4	2020	10.10	TPD-3F:IT-4F	*o*-xylene	Blade-coating	[38]
23.7	2019	7.56	PV2000:$PC_{61}BM$	*o*-xylene	Slot-die coating	[39]
25	2020	10.09	PTB7-Th:CO*i*8DFIC:$PC_{71}BM$	*o*-xylene	Slot-die coating	[19]
25	2021	14.07	PM6:BTP-eC9	chlorobenzene	Blade-coating	[15]
26	2020	12.60	PM6:Y6:$PC_{61}BM$	chloroform	Blade-coating	[21]
30	2019	8.60	PTB7-Th:$PC_{71}BM$:CO*i*8DFIC	chlorobenzene	Slot-die coating	[40]
30	2021	8.10	PM6:BTP-4Cl-12	chlorobenzene	Spin-coating	[41]
36	2021	14.26	PM6:Y6:20% BTO:$PC_{71}BM$	paraxylene	Blade-coating	[16]
40	2021	6.43	PTB7:$PC_{71}BM$	chlorobenzene	Spin-coating	[36]
52	2018	2.20	PBDB-T:ITIC	chlorobenzene	Spin-coating	[42]
54	2021	13.20	PBDB-T-2F:Y6:$PC_{71}BM$	chloroform	Spin-coating	[23]
54.45	2019	6.61	PNTz4T-5MTC:$PC_{71}BM$	*o*-xylene	Bar-coating	[43]
57	2018	3.40	P3HT:ICBA	1,2-dichlorobenzene	R2R printing	[44]
58.5	2020	9.03	PBDB-T:ITIC	chlorobenzene	Blade-coating	[45]
58.5	2020	7.74	BDT-Th10:$PC_{71}BM$	chlorobenzene+*o*-dichlorobenzene	Bar-coating	[46]
60	2018	4.70	P3HT:IDTBR	*o*-methylanisole	Blade-coating	[47]
66	2019	6.10	PF2:$PC_{71}BM$	*o*-xylene	Blade-coating	[48]
80	2019	5.25	SMD2:ITIC-Th	chlorobenzene	Slot-die coating	[24]
85	2020	8.18	PTB7-Th:EH-IDTBR	chlorobenzene	Blade-coating	[49]
204	2020	11.70	PM6:Y6:$PC_{61}BM$	chloroform	Blade-coating	[21]
216	2018	5.63	PBDTTT-EFT:$PC_{71}BM$	chlorobenzene	Blade-coating	[50]
216	2019	7.70	PBDB-T:ITIC:$PC_{71}BM$	chlorobenzene	Blade-coating	[51]
208.4	2009	3.50	–	–	–	[13]
223.5	2009	2.10	–	–	–	[13]
232.8	2008	1.10	–	–	–	[13]
294.5	2011	4.20	–	–	–	[13]
294.5	2012	5.20	–	–	–	[13]
395.9	2012	6.80	–	–	–	[13]
802	2014	8.70	–	–	–	[13]

dong Province (tsqn202103016) and Qilu Young Scholar Program of Shandong University. L. Ding thanks the National Key Research and Development Program of China (2017YFA0206600), the National Natural Science Foundation of China (51922032 and 21961160720), and the open research fund of Songshan Lake Materials Laboratory (2021SLAB-FK02) for financial support.

References

[1] Tong Y, Xiao Z, Du X, et al. Progress of the key materials for organic solar cells. Sci China Chem, 2020, 63, 758

[2] Duan C, Ding L. The new era for organic solar cells: Non-fullerene small molecular acceptors. Sci Bull, 2020, 65, 1231

[3] Cao J, Yi L, Ding L. The origin and evolution of Y6 structure. J Semicond, 2022, 43, 030202

[4] Liu Q, Jiang Y, Jin K, et al. 18% efficiency organic solar cells. Sci Bull, 2020, 65, 272

[5] Qin J, Zhang L, Zuo C, et al. A chlorinated copolymer donor demonstrates a 18.13% power conversion efficiency. J Semicond, 2021, 42, 010501

[6] Jin K, Ou Z, Lixiu Z, et al. A chlorinated lactone polymer donor featuring high performance and low cost. J Semicond, 2022, 43,

050501
[7] Guan W, Yuan D, Wu J, et al. Blade-coated organic solar cells from non-halogenated solvent offer 17% efficiency. J Semicond, 2021, 42, 030502
[8] Cui Y, Xu Y, Yao H, et al. Single-junction organic photovoltaic cell with 19% efficiency. Adv Mater, 2021, 33, 2102420
[9] Jin K, Xiao Z, Ding L. 18.69% power conversion efficiency from organic solar cells. J Semicond, 2021, 42, 060502
[10] Jin K, Xiao Z, Ding L. D18, an eximious solar polymer!. J Semicond, 2021, 42, 010502
[11] Meng X, Jin K, Xiao Z, et al. Side chain engineering on D18 polymers yields 18.74% power conversion efficiency. J Semicond, 2021, 42, 100501
[12] Brabec C J, Distler A, Du X, et al. Material strategies to accelerate OPV technology toward a GW technology. Adv Energy Mater, 2020, 10, 2001864
[13] NREL, Best research-cell efficiency chart, https://www.nrel.gov/pv/cell-efficiency.html (accessed: December 2021)
[14] Dong S, Jia T, Zhang K, et al. Single-component non-halogen solvent-processed high-performance organic solar cell module with efficiency over 14%. Joule, 2020, 4, 2004
[15] Dong X, Jiang Y, Sun L, et al. Large-area organic solar modules with efficiency over 14%. Adv Funct Mater, 2021, 2110209
[16] Chen H, Zhang R, Chen X, et al. A guest-assisted molecular-organization approach for >17% efficiency organic solar cells using environmentally friendly solvents. Nat Energy, 2021, 6, 1045
[17] Park S, Kim T, Yoon S, et al. Progress in materials, solution processes, and long-term stability for large-area organic photovoltaics. Adv Mater, 2020, 32, 2002217
[18] Wang G, Adil M A, Zhang J, et al. Large-area organic solar cells: Material requirements, modular designs, and printing methods. Adv Mater, 2019, 31, 1805089
[19] Wang G, Zhang J, Yang C, et al. Synergistic optimization enables large-area flexible organic solar cells to maintain over 98% PCE of the small-area rigid devices. Adv Mater, 2020, 32, 2005153
[20] Zhang Y, Liu K, Huang J, et al. Graded bulk-heterojunction enables 17% binary organic solar cells *via* nonhalogenated open air coating. Nat Commun, 2021, 12, 4815
[21] Distler A, Brabec C J, Egelhaaf H J. Organic photovoltaic modules with new world record efficiencies. Prog Photovolt Res Appl, 2020, 29, 24
[22] Pan W, Han Y, Wang Z, et al. Over 1 cm^2 flexible organic solar cells. J Semicond, 2021, 42, 050301
[23] Qin F, Sun L, Chen H, et al. 54 cm^2 large-area flexible organic solar modules with efficiency above 13%. Adv Mater, 2021, 33, 2103017
[24] Han Y W, Jeon S J, Lee H S, et al. Evaporation-free nonfullerene flexible organic solar cell modules manufactured by an all-solution process. Adv Energy Mater, 2019, 9, 1902065
[25] Tam K C, Saito H, Maisch P, et al. Highly reflective and low resistive top electrode for organic solar cells and modules by low temperature silver nanoparticle ink. Sol RRL, 2021, 6, 2100887
[26] Cui Y, Yao H, Hong L, et al. Organic photovoltaic cell with 17% efficiency and superior processability. Natl Sci Rev, 2020, 7, 1239
[27] An K, Peng F, Zhong W, et al. Improving photovoltaic parameters of all-polymer solar cells through integrating two polymeric donors. Sci China Chem, 2021, 64, 2010
[28] Liu X, Zheng Z, Wang J, et al. Fluidic manipulating of printable zinc oxide for flexible organic solar cells. Adv Mater, 2021, 34, 2106453
[29] Cui Y, Yao H, Zhang J, et al. Single-junction organic photovoltaic cells with approaching 18% efficiency. Adv Mater, 2020, 32, 1908205
[30] Würfel U, Herterich J, List M, et al. A 1 cm^2 organic solar cell with 15.2% certified efficiency: Detailed characterization and identification of optimization potential. Sol RRL, 2021, 5, 2000802
[31] Han Y, Chen X, Wei J, et al. Efficiency above 12% for 1 cm^2 flexible organic solar cells with Ag/Cu grid transparent conducting electrode. Adv Sci, 2019, 6, 1901490
[32] Sun R, Wu Q, Guo J, et al. A layer-by-layer architecture for printable organic solar cells overcoming the scaling lag of module efficiency. Joule, 2020, 4, 407
[33] Meng X, Zhang L, Xie Y, et al. A general approach for lab-to-manufacturing translation on flexible organic solar cells. Adv Mater, 2019, 31, 1903649
[34] Zhang K, Chen Z, Armin A, et al. Efficient large area organic solar cells processed by blade-coating with single-component green solvent. Sol RRL, 2018, 2, 1700169
[35] Mao L, Luo B, Sun L, et al. Writable and patternable organic solar cells and modules inspired by an old chinese calligraphy tradition. Mater Horizons, 2018, 5, 123
[36] Jeong J H, Jahandar M, Prasetio A, et al. Multi-dimensional interfacial engineering for a practical large-area transparent flexible organic photovoltaics. Chem Eng J, 2021, 419, 129672
[37] Jia Z, Chen Z, Chen X, et al. 19.34 cm^2 large-area quaternary organic photovoltaic module with 12.36% certified efficiency. Photonics Res, 2021, 9, 324
[38] Liao C Y, Chen Y, Lee C C, et al. Processing strategies for an organic photovoltaic module with over 10% efficiency. Joule, 2020, 4, 189
[39] Chang Y M, Liao C Y, Lee C C, et al. All solution and ambient processable organic photovoltaic modules fabricated by slot-die coating and achieved a certified 7.56% power conversion efficiency. Sol Energy Mater Sol Cells, 2019, 202, 110064
[40] Lee J, Seo Y H, Kwon S N, et al. Slot-die and roll-to-roll processed single junction organic photovoltaic cells with the highest efficiency. Adv Energy Mater, 2019, 9, 1901805
[41] Han Y W, Lee H S, Moon D K. Printable and semitransparent nonfullerene organic solar modules over 30 cm^2 introducing an energy-level controllable hole transport layer. ACS Appl Mater Interfaces, 2021, 13, 19085
[42] Mao L, Sun L, Luo B, et al. Patching defects in the active layer of large-area organic solar cells. J Mater Chem A, 2018, 6, 5817
[43] Rasool S, Vu D V, Song C E, et al. Room temperature processed highly efficient large-area polymer solar cells achieved with molecular engineering of copolymers. Adv Energy Mater, 2019, 9, 1900168
[44] Apilo P, Välimäki M, Po R, et al. Fully roll-to-roll printed P3HT/indene-C60-bisadduct modules with high open-circuit voltage and efficiency. Sol RRL, 2018, 2, 1700160
[45] Park S H, Park S, Lee S, et al. Developement of highly efficient large area organic photovoltaic module: Effects of nonfullerene acceptor. Nano Energy, 2020, 77, 105147
[46] Park S H, Park S, Kurniawan D, et al. Highly efficient large-area organic photovoltaic module with a 350 nm thick active layer using a random terpolymer donor. Chem Mater, 2020, 32, 3469
[47] Strohm S, Machui F, Langner S, et al. P3HT: Non-fullerene acceptor based large area, semi-transparent PV modules with power conversion efficiencies of 5%, processed by industrially scalable methods. Energy Environ Sci, 2018, 11, 2225
[48] Ibraikulov O A, Wang J, Kamatham N, et al. ITO-free organic photovoltaic modules based on fluorinated polymers deposited from non-halogenated solution: A major step toward large-scale module production. Sol RRL, 2019, 3, 1900273

[49] Wang D, Zhou G, Li Y, et al. High-performance organic solar cells from non-halogenated solvents. Adv Funct Mater, 2021, 32, 2107827
[50] Huang K M, Wong Y Q, Lin M C, et al. Highly efficient and stable organic solar cell modules processed by blade coating with 5.6% module efficiency and active area of 216 cm^2. Prog Photovolt, 2019, 27, 264
[51] Huang K M, Lin C M, Chen S H, et al. Nonfullerene polymer solar cell with large active area of 216 cm^2 and high power conversion efficiency of 7.7%. Sol RRL, 2019, 3, 1900071

Min Li received her BE from Xiangtan University in 2021. She is currently pursuing master degree in Shandong University under the supervision of Prof. Xiaoyan Du. Her research focuses on organic solar cells.

Jilin Wang received his PhD in 2014 form Wuhan University of Technology under the supervision of Professor Weimin Wang. He joined Guilin University of Technology in 2015. Currently, he is an associate professor in Fei Long Group. His research focuses on optoelectronic materials and devices.

Liming Ding got his PhD from University of Science and Technology of China (was a joint student at Changchun Institute of Applied Chemistry, CAS). He started his research on OSCs and PLEDs in Olle Inganäs Lab in 1998. Later on, he worked at National Center for Polymer Research, Wright-Patterson Air Force Base and Argonne National Lab (USA). He joined Konarka as a Senior Scientist in 2008. In 2010, he joined National Center for Nanoscience and Technology as a full professor. His research focuses on innovative materials and devices. He is RSC Fellow, the nominator for Xplorer Prize, and the Associate Editor for Journal of Semiconductors.

Xiaoyan Du started her research on OSCs in Liming Ding Group as a MS student in 2010–2013. She received her PhD under the supervision of Prof. Rainer H. Fink and Prof. Christoph J. Brabec in 2017 from Friedrich-Alexander Universität Erlangen-Nürnberg (FAU) in Germany. In 2017–2021, she was a postdoc in FAU and did photo-degradation and voltage loss studies. In 2020–2021, she was a research scientist in Helmholtz-Institute Erlangen-Nürnberg doing research on high-throughput methods. Now she is a professor in Shandong University. Her research focuses on solution-processed photovoltaic materials and devices.